How to cite: *Angew. Chem. Int. Ed.* **2021**, *60*, 360–365
International Edition: doi.org/10.1002/anie.202010404
German Edition: doi.org/10.1002/ange.202010404

Germanane

Synthesis of 2D Germanane (GeH): a New, Fast, and Facile Approach

Theodosis Giousis, Georgia Potsi, Antonios Kouloumpis, Konstantinos Spyrou, Yiannis Georgantas, Nikolaos Chalmpes, Konstantinos Dimos, Myrsini-Kiriaki Antoniou, Georgios Papavassiliou, Athanasios B. Bourlinos, Hae Jin Kim, Vijay Kumar Shankarayya Wadi, Saeed Alhassan, Majid Ahmadi, Bart J. Kooi, Graeme Blake, Daniel M. Balazs, Maria A. Loi, Dimitrios Gournis, and Petra Rudolf**

Abstract: *Germanane (GeH), a germanium analogue of graphane, has recently attracted considerable interest because its remarkable combination of properties makes it an extremely suitable candidate to be used as 2D material for field effect devices, photovoltaics, and photocatalysis. Up to now, the synthesis of GeH has been conducted by substituting Ca by H in a β-$CaGe_2$ layered Zintl phase through topochemical deintercalation in aqueous HCl. This reaction is generally slow and takes place over 6 to 14 days. The new and facile protocol presented here allows to synthesize GeH at room temperature in a significantly shorter time (a few minutes), which renders this method highly attractive for technological applications. The GeH produced with this method is highly pure and has a band gap (E_g) close to 1.4 eV, a lower value than that reported for germanane synthesized using HCl, which is promising for incorporation of GeH in solar cells.*

Introduction

The discovery of graphene,[1] in 2004 was trailblazing for the new field of two-dimensional (2D) materials that exhibit remarkable mechanical, thermal and (opto)electronic properties, often surpassing those of their bulk counterparts.[2] Since then a widespread effort has been devoted to the fabrication of 2D solids, their characterization and the exploration of how to exploit them for (opto)electronic applications,[3] as energy materials[4] or catalysts.[5] A particular place in this research landscape is occupied by the other group VI honeycomb structures, the so-called Xenes (silicene, germanene and stanene), and their Hydrogen- or ligand-functionalized derivatives, called Xanes. While Xenes and Xanes have been fabricated by molecular beam epitaxy, germanane is the only one for which a chemical synthesis has been developed.

Germanane or polygermyne was first reported in 2000 by Vogg et al. who studied the topochemical reaction of $CaGe_2$ with HCl at low temperature resulting in a crystalline layered compound isomorphic to polysilyne.[6] Later, Bianco et al., using a similar synthetic method, reported the exfoliation of GeH and studied some of the properties of germanane such as thermal stability and the optical band gap.[7] This analogue of graphane exhibits a direct band gap of approximately 1.59 eV[8] and its predicted charge carrier mobility is $> 18\,000\ cm^2 V^{-1} s^{-1}$, five times higher than that of crystalline germanium. These characteristics hold great promise for electronic and optoelectronic applications and recently we reported the first realization of germanane field effect

[*] T. Giousis, Dr. G. Potsi, Dr. A. Kouloumpis, Dr. K. Spyrou, Y. Georgantas, N. Chalmpes, Dr. K. Dimos, Dr. M.-K. Antoniou, Prof. D. Gournis
Department of Materials Science & Engineering, University of Ioannina
45110 Ioannina (Greece)
E-mail: dgourni@cc.uoi.gr

T. Giousis, Dr. G. Potsi, Dr. A. Kouloumpis, Y. Georgantas, Dr. M. Ahmadi, Prof. B. J. Kooi, Dr. G. Blake, Dr. D. M. Balazs, Prof. M. A. Loi, Prof. P. Rudolf
Zernike Institute for Advanced Materials, University of Groningen
Nijenborgh 4, 9747 AG Groningen (The Netherlands)
E-mail: p.rudolf@rug.nl

Dr. G. Papavassiliou
Institute of Nanoscience and Nanotechnology, NCSR "DEMOKRITOS"
15310 Ag. Paraskevi-Attikis, Athens (Greece)

Prof. A. B. Bourlinos
Department of Physics, University of Ioannina
45110 Ioannina (Greece)

Dr. H. J. Kim
Nano-Bio Electron Microscopy Research Group, Korea Basic Science Institute
Yuseong-gu, Daejeon (Republic of Korea)

V. K. S. Wadi, Prof. S. Alhassan
Department of Chemical Engineering, Khalifa University of Science and Technology, The Petroleum Institute
PO Box 2533, Abu Dhabi (United Arab Emirates)

Dr. G. Potsi, Dr. A. Kouloumpis
current address: Department of Materials Science and Engineering, Cornell University
Ithaca, NY, 14853 (USA)

Y. Georgantas
current address: Department of Materials, National Graphene Institute, Henry Royce Institute, University of Manchester
Oxford Road, Manchester, M13 9PL (United Kingdom)

Dr. K. Dimos
current address: Department of Materials Science, University of Patras
GR-26504 Patras (Greece)

Supporting information and the ORCID identification number(s) for the author(s) of this article can be found under: https://doi.org/10.1002/anie.202010404.

transistors, fabricated from multilayer single crystal flakes, which demonstrated transport in both electron and hole doped regimes, with an on/off current ratio of up to $10^5(10^4)$ and carrier mobilities of 150 $cm^2V^{-1}s^{-1}$ (70 $cm^2V^{-1}s^{-1}$) at 77 K (room temperature).[9]

Moreover, in a separate study[10] we found evidence for a highly conductive metallic state that develops with the dehydrogenation during heating, a process, which seems to transform germanane thin flakes into multilayer germanene. These results as well as many other recently proposed applications of germanane[8a,11] and germanene[12] in (opto)-electronics, energy production and storage as well as in (photo)catalysis leave no doubt that a large scale, low cost and fast synthesis for very high quality and thermally stable germanane flakes is urgently required in order to fully explore the scientific and technological potential of 2D germanium-based materials.

Responding to this quest, here we report a new facile approach for the production of high purity germanane flakes, which is significantly faster than the time consuming methods published to date.[7,13,14] In fact, these synthetic protocols, which rely on the use of various acids (HCl, HBr, HI or acetic acid) at different temperatures (from −40 to 25 °C), require reaction times between 5 to 14 days, while our method delivers the product in a few minutes.

Results and Discussion

Our approach employs an aqueous HF solution (38 % w/w) for the topotatic deintercalation of β-$CaGe_2$ at room temperature in only a few minutes (or even a few seconds) to yield high quality GeH. The details of the method are explained below. β-$CaGe_2$ crystals (Figure 1 a) react instantaneously with aqueous HF according to the reaction:

$$CaGe_2 + 2\,HF \rightarrow CaF_2 + 2\,GeH \quad (1)$$

A product with a platelet-like morphology was formed, as shown in the scanning electron microscopy (SEM) image presented in Figure 1 b top left panel. The several μm long flakes are fully covered with calcium fluoride, the byproduct of the reaction, as evident from the energy-dispersive X-ray spectroscopy (EDX) analysis (Figure 1 b bottom left panel). To remove the residual CaF_2, the material was treated with a saturated aqueous solution of ethylenediaminetetraacetic acid (EDTA); EDTA is highly water-soluble and acts as a chelating agent that allows to extract the residual Ca^{2+} from the sample. In order to understand the role of fluorine during the reaction, one must consider that the electronegativity of fluorine is higher than that of other halogens.[15] In this context, fluorine is more electronegative than Ge in $CaGe_2$, causing the fast formation of the calcium halide by-product and hence the formation of germanane. This is in agreement with the findings of Ramachandran et al.,[16] who reported that during the topotactic deintercalation of the Zintl phase of $CaSi_2$, the HF reactivity is very high, while the use of HCl instead of HF results in a different solubility of the calcium halides formed. The formation of insoluble solid CaF_2 during etching is instant and thus helps to pull the reaction toward the product side due to the removal of CaF_2 from the system according to Le Chatelier's principle.

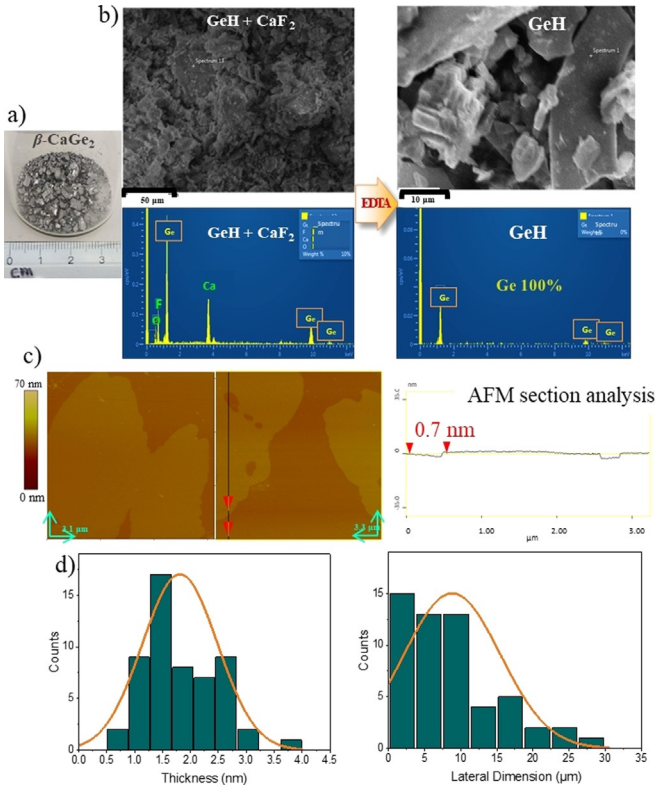

Figure 1. a) Small crystals of the synthesized β-$CaGe_2$ Zintl Phase. b) SEM images (and corresponding EDX spectra) of germanane before and after treatment with EDTA. c) AFM images (including height profile analysis) of exfoliated germanane sheets prepared by drop-casting dilute suspensions (in ethanol) on Si-wafers. d) statistical analysis of the thickness and lateral dimensions of 55 GeH flakes as deduced from AFM images.

Finally, the product was filtered and washed several times with water and methanol. After this treatment, SEM and EDX analysis (Figure 1 b right panels) revealed a layered germanium-based material, free of any residual salt as proven by the absence of Ca and F signals in the EDX spectrum (Figure 1 b bottom right panel). The product is highly dispersible in ethanol and DMF and this property can be exploited for liquid exfoliation of individual germanane sheets. In fact, atomic force microscopy (AFM) analysis of drop-casted films revealed a substrate covered by single layers of germanane[7] with a thickness of about 7 Å (Figure 1 c and d; for additional examples see Supporting Information) as well as few-layer germanane flakes (with a thickness of 2–3 nm). The germanane layers showed a distribution of various sizes (see Figure 1 d), most of them measured between 5 and 10 μm but a few reached up to 15–25 μm.

The powder sample contained many black granular pieces of an approximate size of 0.1 mm (for details see SI). As presented in Figure 2, X-ray diffraction (XRD) showed that these pieces are single crystals, although with considerable disorder in the layer stacking direction as described below.

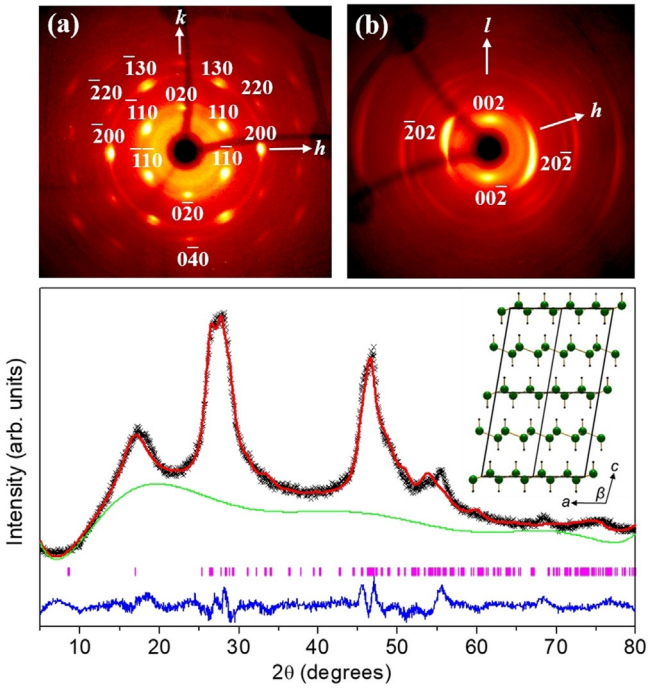

Figure 2. X-ray diffraction pattern of germanane crystallites. *Top panels:* a) *hk*0 and b) *h*0*l* reciprocal lattice images reconstructed from raw single-crystal XRD data. *Bottom panel:* Observed (black data points), fitted (red line) and difference (blue line) XRD profiles. The green line indicates a polynomial fit to the background. Markers underneath the pattern indicate peak positions allowed by symmetry. The inset shows the refined crystal structure viewed along the *b*-axis.

The unit cell at 100 K is monoclinic with approximate lattice parameters $a \approx 7.0$ Å, $b \approx 4.0$ Å, $c \approx 11.7$ Å, $\beta \approx 107°$. Reciprocal lattice sections reconstructed from the raw data (Figure 2 top panels) show that the reflection condition $h + k = 2n$ is obeyed, consistent with a C-centered lattice. Although the *hk*0 plane is relatively well defined, along the reciprocal *l*-axis only the 002 spot can be clearly distinguished. Other peaks in the *h*0*l* plane are strongly streaked or present as rings of weak intensity, which implies considerable disorder. The poor data quality prevented full solution of the structure.

The structure was further investigated at 295 K using powder XRD on a larger portion of the bulk sample. No peaks from elemental germanium are observed, demonstrating that the current synthesis method has the advantage over the method involving HCl (described in Ref. [9]) of producing only GeH. The main features of the XRD pattern could be fitted using a starting model comprising the 100 K unit cell parameters, which were then refined, and the Ge positions that were obtained from our previous structure determination on a sample prepared by the HCl-based method.[9] The atomic positions of Ge were refined using soft constraints, keeping the Ge-Ge bond distances close to 2.43 Å (the average bond distance in the germanane structure determined in Ref. [9]). The refined atomic parameters are listed in Table 1 and the fitted XRD profile is shown in Figure 2 (bottom panel) with an *ac*-plane view of the structure (H atoms were generated automatically by geometrical considerations and not refined).

Table 1: Partially refined atomic coordinates and isotropic displacement factors for germanane at 295 K. Hydrogen positions were generated by geometrical considerations and not refined. Space group *C*2: $a = 6.789(10)$ Å, $b = 4.035(5)$ Å, $c = 11.24(4)$ Å, $\beta = 105.5(2)°$.

Atom	*x*	*y*	*Z*	U_{iso} [Å^2]
Ge1	0.6547(10)	0.382(3)	0.9642(10)	0.058(2)
Ge2	0.6934(11)	0.015(3)	0.5359(12)	0.058(2)
H1	0.6172	0.3820	0.8241	
H2	0.7344	0.0150	0.6796	

The crystal structure determined from powder XRD is similar to that of the sample prepared using HCl,[9] although with a significantly larger β angle (105.5° versus 102.2°). As shown in Figure S2, this angle is associated with the lateral displacement of successive GeH layers. For the 2H polymorph of GeH reported by Bianco et al. the lateral displacements of successive layers are equal and opposite, giving a β angle of precisely 90° and allowing the structure to be described in a 2-layer hexagonal unit cell. The in-plane structure is similar in all three samples, where Ge atoms form 6-membered rings in the "chair" configuration. We note that the precursor phase, β-$CaGe_2$, adopts a 6-layer rhombohedral unit cell with $a = 3.987$ Å, $c = 30.58$ Å.[17] This can alternatively be described in a monoclinic unit cell with $a' = 6.906$ Å, $b' = 3.987$ Å, $c' = 10.45$ Å, $\beta = 102.73°$, thus the Ge-sublattice is essentially retained in our present GeH sample with an expansion of the interlayer distance by ≈ 0.4 Å. Although EDX data (Figure 1) gave no evidence for the presence of residual Ca, we tested whether the different β angles in the present sample and the sample produced employing HCl might result from different residual amounts of Ca cations remaining between the GeH layers. Refinements using a model incorporating Ca were inconclusive—difficulties in precisely modelling the intensities and profiles of the broad peaks (Figure 2) do not allow us to confirm or discount the presence of minute amounts of Ca (too small to be detected spectroscopically). The broadness of all the peaks suggests that the correlation length of crystalline order in the powder is rather short. The XRD pattern also exhibits a high background, suggesting that part of the sample is amorphous. These observations are confirmed by Transmission Electron Microscopy (TEM) analysis. The TEM images shown in Figure 3a and b indicate that the product has a layered morphology, with individual layers having low contrast compared to the TEM support grid. The selected area electron diffraction pattern, taken orthogonally to the layers, is shown as an inset in Figure 3a. Strikingly, clear diffraction spots arranged in a 6-fold symmetry pattern are observed. The measurements are in agreement with the data extracted from the XRD analysis along *z*-axis of the germanane flakes, shown in Figure 2a. These TEM images were recorded with a low e-beam dose of 5.0 e nm^{-2} s^{-1}. At higher e-beam doses the material was no longer stable but a phase transition to cubic Ge (with space group $Fd\bar{3}m$) and to a hexagonal Ge phase were observed (see SI Figure S4). The lattice planes of cubic Ge (c-Ge) are observed in the SAED pattern shown in Figure 3a as well.

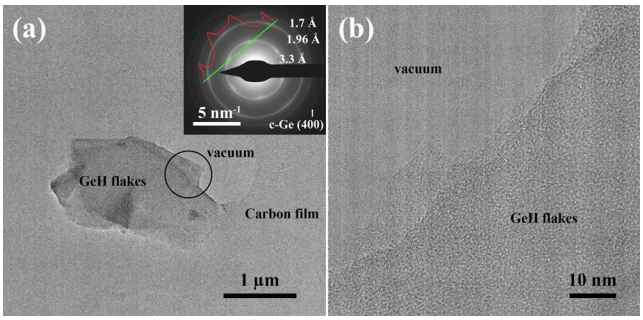

Figure 3. Bright field TEM images of two different GeH flakes suspended on carbon film. Inset in "a" illustrates the corresponding selected area electron diffraction (SAED) pattern of GeH flakes recorded from the area circled in black. The measured d-spacing of 3.3 Å corresponds to {110} and {020} lattice planes, while the measured d-spacing of 1.96 Å corresponds to {200} and {130} lattice planes. The SAED pattern is indexed along the [001] axis. The line intensity profile along the green line indicates higher intensities for the inner planes (3.3 Å) than for the outer planes (1.96 Å) for this multilayer GeH flake.

FT-IR, Raman and ^{1}H MAS NMR spectroscopic measurements were performed in order to confirm the presence of hydrogen in the final product and to further elucidate its structure as well as to study its thermal stability. Figure 4a shows ^{1}H MAS NMR spectra of the GeH sample at room temperature, as well as upon thermal treatment at various temperatures (up to 275 °C). The sample was heated for 2 h at each temperature, subsequently cooled to room temperature in vacuum, and then shielded into the sample holder for performing the NMR experiment. Before any heat treatment, the ^{1}H MAS NMR spectrum is dominated by a peak at

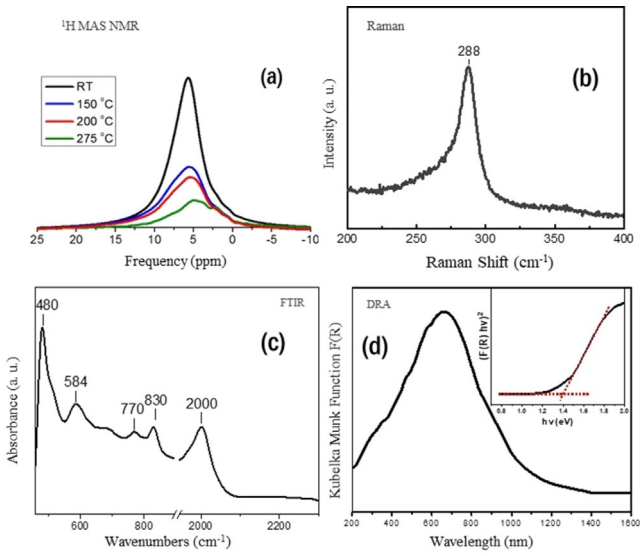

Figure 4. Spectroscopic characterization of GeH: a) ^{1}H MAS NMR of GeH sample before and after thermal treatment at various temperatures (150, 200 and 275 °C). b) Raman and c) FT-IR spectrum of GeH. d) Diffuse reflectance absorbance (DRA) spectrum plotted as Kubelka–Munk function versus wavelength; inset: Tauc-plot analysis of the Kubelka–Munk function for the allowed direct transition.

5.6 ppm, attributed to Ge-H; a very small quantity of adsorbed water (at 4.8 ppm) cannot be excluded. A Ge-H resonance at 5.16 ppm has been previously reported for 2,2′diphenylene germanane.[18] At elevated treatment temperatures part of the GeH hydrogen dissociates, as deduced from the strong decrease of the signal. However, a large part of the signal persists not only upon heating at 200 °C but even after annealing at the highest temperature of 275 °C. At the same time, a small shift of the peak towards lower chemical shift values is observed, which is indicative of a slightly more effective electron shielding. In the Raman spectrum of the synthesized powder (Figure 4b) a characteristic peak associated with Ge–H bonds[9] is observed at 288 cm^{-1} thus confirming the composition of the studied material. This peak corresponds in fact to the E_{2g} in-plane Raman mode for the chair configuration of germanane.[19] The position of the A_{1g} band cannot be identified in our data, probably because polarization phenomena, to which the A_{1g} band is sensitive due to the random orientation of the flakes of the material (powder sample), cause a further intensity reduction of the already weak peak.[20] Moreover the absence of the characteristic CaF_2 peak[21] at 321 cm^{-1} agrees with the XRD and EDX results in confirming the purity of the material and the successful removal of salts through EDTA treatment. The FT-IR spectrum of β-$CaGe_2$ (Figure S2) showed very broad features and no distinctive bands could be identified in the 400–4000 cm^{-1} region, in agreement with previous reports.[22] The FT-IR spectrum of germanane (Figure 4c) shows a strong peak due to the Ge-H stretching vibration at 2000 cm^{-1}, as well as the signature of the wagging modes[7,23] of Ge-H at 480 and 584 cm^{-1}. In addition, weak peaks at 770 and 830 cm^{-1} are also present, and correspond to H-Ge-H bending modes from neighbouring germanium atoms at the edges of the crystalline germanane layers and/or Ge vacancies within the layered germanane lattice.[7] FT-IR spectroscopy hence clearly confirms the hydrogen termination of the germanium atoms.

The UV/Vis-NIR diffuse reflectance spectrum of germanane plotted as Kubelka–Munk function F(R∞) versus wavelength is shown in Figure 4d and demonstrates that the sample absorbs strongly in the whole visible light region. The Tauc-Plot analysis of the Kubelka–Munk function versus energy is presented in the inset of Figure 4d. Drawing the tangent line to the point of inflection, the band gap (E_g) is determined as the point of intersection with the zero of $(F(R\infty)\,E)^2$ and gives $E_g = 1.4$ eV for our material. This value is lower than that reported in the literature for the 2H GeH synthesized using HCl[7,9,14] This is not unexpected considering that Luo et al. have shown that the band gap of GeH depends on the number of layers in the unit cell, the stacking sequence and interlayer distance[24] in the crystal. The different value of band gap as compared to GeH synthesized using HCl is therefore very likely due to the different lattice parameters. In addition, given the higher disorder in our GeH crystals, an effect of localized states inside the band gap cannot be excluded. The lower E_g makes the material more attractive for use as a solar cell semiconductor; in fact, in order to absorb as much of the solar spectrum as possible and achieve the maximum solar conversion efficiency, a band gap close to the Shockley–Queiser limit of 1.34 eV is required.[25]

On the other hand, the very small effective masses present in small band gap materials make them suitable candidates for the observation of quantum confinement effects at larger dimensions than in materials with larger effective mass and wider band gap.[26] Moreover, the lower E_g value renders the material suitable for photodetection at lower energies without the need to synthesize alloyed Zintl phases that are already reported in literature[27] and usually lack homogeneity.

Conclusion

In conclusion, hydrogen-terminated germanane was synthesized by topotatic deintercalation of β-$CaGe_2$ in aqueous HF solution at room temperature for a few minutes. A product with a platelet-like morphology was formed upon reaction, fully covered with calcium fluoride salt, the by-product of the reaction. The latter was efficiently removed when the material was treated with a saturated aqueous solution of EDTA. FT-IR, Raman and ^{1}H MAS NMR measurements confirmed the presence of the Ge−H bonds in the final product, EDX could not detect any residual salt in the GeH crystallites. The resulting high quality GeH has a crystal structure determined from powder XRD that is similar to that of samples prepared using HCl, although with a significantly larger β angle (105.5° versus 102.2°). No diffraction peaks from elemental germanium were observed, demonstrating the advantage of this new synthesis method over the method involving HCl. After liquid exfoliation, AFM analysis of the drop-casted suspension revealed the presence of single layers of germanane with a thickness of about 7 Å. When the crystallites were heated to elevated temperatures, part of the GeH hydrogen dissociates, as deduced from the strong decrease in ^{1}H MAS NMR signal; however, a considerable part of the signal is still observed upon heating to 275 °C. From UV/Vis-NIR diffuse reflectance measurements a band gap (E_g) of 1.4 eV is deduced. This value is considerably lower than that reported in the literature for germanane synthesized using HCl (1.59 eV), making the material attractive for photovoltaic applications.

Experimental Section

Synthetic protocol. Germanane was synthesized by topotatic deintercalation of β-$CaGe_2$ in aqueous HF solution (Merck, 38–40 % w/w) at room temperature. (**Caution! HF can cause severe burns. Contact with the skin must be avoided and the compound should be handled only in a well-ventilated fume hood. Appropriate safety precautions should be taken when working with HF**). The initial phase of β-$CaGe_2$ was synthesized by sealing amounts of calcium (granular Ca with purity 99 % from Sigma–Aldrich) and germanium (Ge powder with purity 99.999 %, Sigma–Aldrich) in the ratio 1:1.75 in a cylindrical alumina crucible (external diameter of 11 mm) enclosed in an evacuated fused quartz tube (internal diameter of 12 mm). Mixing of the two metals and filling of the crucible were performed in a glove box under nitrogen atmosphere. The sealed quartz tube was then placed in a box furnace and the following temperature profile was employed: (1) heating to 1025 °C at a rate of 8.3 °C min^{-1}; (2) annealing at 1025 °C for 20 h; (3) slow cooling to 500 °C at a rate of 0.1 °C min^{-1} and finally cooling down to room temperature at a rate of 0.2 °C min^{-1}. Small crystals (2–6 mm) of $CaGe_2$ were collected, (Figure 1 a), placed in a polyethylene bottle and treated with an aqueous HF solution 38–40 % w/w at room temperature under stirring for 2–3 min. Diluting HF and prolonging the reaction time does not result in the same material (see Supporting Information). The product was then washed several times with MilliQ water, centrifuged and air-dried. To remove the residual CaF_2, the material was then treated with a saturated aqueous solution of ethylenediaminetetraacetic acid disodium salt dihydrate (EDTA-Na_2, Sigma–Aldrich, ACS reagent 99.0–101.0 %) for 30 min (while stirring), centrifuged and washed four times with MilliQ water and one time with methanol to speed up the drying process at ambient conditions. The final product consists of black crystallites of an approximate size of 0.1 mm (for details see SI). For the liquid exfoliation, GeH dispersions 0.04 mg mL^{-1} in ethanol (Sigma–Aldrich, used as received) were sonicated for 15 min using a probe ultrasonicator (Ultrasonicator biobase UCD150L, 150 W) and centrifuged for 10 min at 1000 rpm to purify by removing any remaining aggregates/non-exfoliated crystallites.

Acknowledgements

This work received support from the "Top Research School" programme of the Zernike Institute for Advanced Materials under the Bonus Incentive Scheme (BIS) of the Netherlands' Ministry of Education, Science, and Culture. We acknowledge support for this work by the project MIS 5002772, implemented under the Action "Reinforcement of the Research and Innovation Infrastructure", funded by the Operational Programme "Competitiveness, Entrepreneurship and Innovation" (NSRF 2014-2020) and co-financed by Greece and the European Union (European Regional Development Fund). NC gratefully acknowledges the IKY Foundation for the financial support. This research was co-financed by Greece and the European Union (European Social Fund—ESF) through the Operational Programme "Human Resources Development, Education and Lifelong Learning" in the context of the project "Strengthening Human Resources Research Potential via Doctorate Research" (MIS-5000432), implemented by the State Scholarships Foundation (IKY).

Conflict of interest

The authors declare no conflict of interest.

Keywords: germanane · semiconductors · synthesis · topotatic de-intercalation · two-dimensional materials

[1] a) K. S. Novoselov, A. K. Geim, S. V. Morozov, D. Jiang, M. I. Katsnelson, I. V. Grigorieva, S. V. Dubonos, A. A. Firsov, *Nature* **2005**, *438*, 197–200; b) K. S. Novoselov, A. K. Geim, S. V. Morozov, D. Jiang, Y. Zhang, S. V. Dubonos, I. V. Grigorieva, A. A. Firsov, *Science* **2004**, *306*, 666–669.

[2] J. D. Fowler, M. J. Allen, V. C. Tung, Y. Yang, R. B. Kaner, B. H. Weiller, *ACS Nano* **2009**, *3*, 301–306.

[3] a) K. S. Novoselov, D. Jiang, F. Schedin, T. J. Booth, V. V. Khotkevich, S. V. Morozov, A. K. Geim, *Proc. Natl. Acad. Sci. USA* **2005**, *102*, 10451–10453; b) V. W. Brar, M. C. Sherrott, D. Jariwala, *Chem. Soc. Rev.* **2018**, *47*, 6824–6844.

[4] P. Zhang, F. Wang, M. Yu, X. Zhuang, X. Feng, *Chem. Soc. Rev.* **2018**, *47*, 7426 – 7451.
[5] D. Deng, K. S. Novoselov, Q. Fu, N. Zheng, Z. Tian, X. Bao, *Nat. Nanotechnol.* **2016**, *11*, 218 – 230.
[6] G. Vogg, M. S. Brandt, M. Stutzmann, *Adv. Mater.* **2000**, *12*, 1278 – 1281.
[7] E. Bianco, S. Butler, S. Jiang, O. D. Restrepo, W. Windl, J. E. Goldberger, *ACS Nano* **2013**, *7*, 4414 – 4421.
[8] a) L. C. Lew Yan Voon, E. Sandberg, R. S. Aga, A. A. Farajian, *Appl. Phys. Lett.* **2010**, *97*, 163114; b) M. Houssa, E. Scalise, K. Sankaran, G. Pourtois, V. V. Afanas'ev, A. Stesmans, *Appl. Phys. Lett.* **2011**, *98*, 223107.
[9] B. N. Madhushankar, A. Kaverzin, T. Giousis, G. Potsi, D. Gournis, P. Rudolf, G. R. Blake, C. H. van der Wal, B. J. van Wees, *2D Mater. 2D Materials* **2017**, *4*, 021009.
[10] Q. Chen, L. Liang, G. Potsi, P. Wan, J. Lu, T. Giousis, E. Thomou, D. Gournis, P. Rudolf, J. Ye, *Nano Lett.* **2019**, *19*, 1520 – 1526.
[11] M. Niu, D. Cheng, D. Cao, *Sci. Rep.* **2014**, *4*, 4810.
[12] N. Liu, G. Bo, Y. Liu, X. Xu, Y. Du, S. X. Dou, *Small* **2019**, *15*, 1805147.
[13] S. Jiang, E. Bianco, J. E. Goldberger, *J. Mater. Chem. C* **2014**, *2*, 3185 – 3188.
[14] Z. Liu, Z. Lou, Z. Li, G. Wang, Z. Wang, Y. Liu, B. Huang, S. Xia, X. Qin, X. Zhang, Y. Dai, *Chem. Commun.* **2014**, *50*, 11046 – 11048.
[15] R. Yaokawa, T. Ohsuna, T. Morishita, Y. Hayasaka, M. J. S. Spencer, H. Nakano, *Nat. Commun.* **2016**, *7*, 10657.
[16] R. Ramachandran, D. Johnson-McDaniel, T. T. Salguero, *Chem. Mater.* **2016**, *28*, 7257 – 7267.
[17] P. H. Tobash, S. Bobev, *J. Solid State Chem.* **2007**, *180*, 1575 – 1581.
[18] I. M. A. Drummond, PhD Thesis thesis, McMaster University, **1970**.
[19] J. Rivera-Julio, A. González-García, R. González-Hernández, W. López-Pérez, F. M. Peeters, A. D. Hernández-Nieves, *J. Phys. Condens. Matter* **2019**, *31*, 075301.
[20] X. Zhang, Q.-H. Tan, J.-B. Wu, W. Shi, P.-H. Tan, *Nanoscale* **2016**, *8*, 6435 – 6450.
[21] P. Dolcet, A. Mambrini, M. Pedroni, A. Speghini, S. Gialanella, M. Casarin, S. Gross, *RSC Adv.* **2015**, *5*, 16302 – 16310.
[22] J. Sturala, J. Luxa, S. Matějková, Z. Sofer, M. Pumera, *Nanoscale* **2019**, *11*, 19327 – 19333.
[23] S. Jiang, S. Butler, E. Bianco, O. D. Restrepo, W. Windl, J. E. Goldberger, *Nat .Commun.* **2014**, *5*, 3389.
[24] X. Luo, E. Zurek, *J. Phys. Chem. C* **2016**, *120*, 793 – 800.
[25] a) C. Wadia, A. P. Alivisatos, D. M. Kammen, *Environ. Sci. Technol.* **2009**, *43*, 2072 – 2077; b) S. Rühle, *Solar Energy* **2016**, *130*, 139 – 147.
[26] T. C. McGill, D. A. Collins, *Semicond. Sci. Technol.* **1993**, *8*, S1 – S5.
[27] M. Q. Arguilla, S. Jiang, B. Chitara, J. E. Goldberger, *Chem. Mater.* **2014**, *26*, 6941 – 6946.

Manuscript received: July 29, 2020
Revised manuscript received: August 21, 2020
Accepted manuscript online: August 31, 2020
Version of record online: November 3, 2020

